Electronic Supplementary Material (ESI) for CrystEngComm.

Synthesis of highly luminescent Mn-doped $CsPbCl_3$ nanoplatelets for light-emitting diodes

Zhuo Chen[a,b], *Lvming Dong*[a], *Cheng Zhou*[a], *Binze Zhou*[c], *Zhi Zheng*[d], *Rong Chen*[c], *Jianfeng Zang*[a,b,*]

[a] School of Optical and Electronic Information and Wuhan National Laboratory for Optoelectronics, Huazhong University of Science and Technology, Wuhan 430074, China

[b] Innovation Institute, Huazhong University of Science and Technology, Wuhan 430074, China

[c] State Key Laboratory of Digital Manufacturing Equipment and Technology, School of Mechanical Science and Engineering, Huazhong University of Science and Technology, Wuhan, 430074, China

[d] State Key Laboratory of Materials Processing and Die & Mould Technology, School of Materials Science and Engineering, Huazhong University of Science and Technology, Wuhan, 430074, China

* Correspondence should be given to: jfzang@hust.edu.cn (J.Z.)

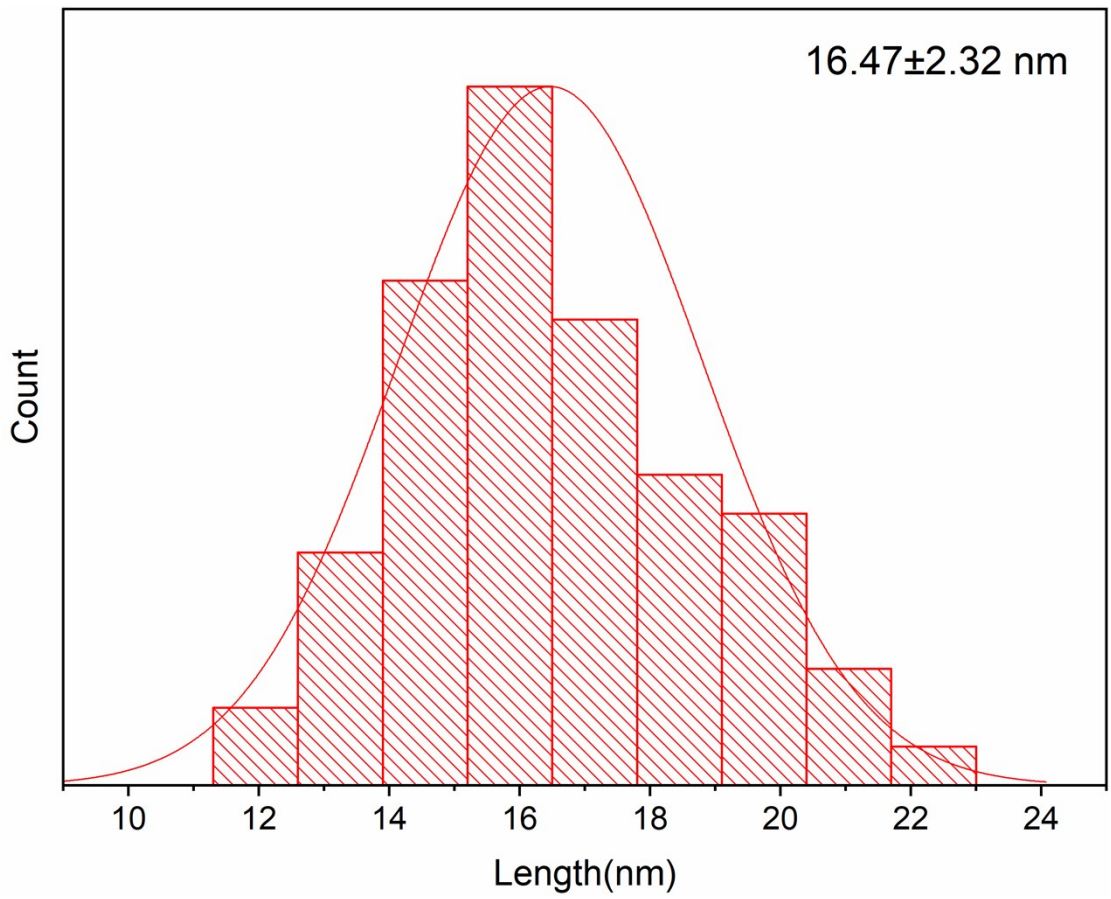

Figure S1. The length distribution of Mn-doped $CsPbCl_3$ NPLs at Mn-Pb feed ratio of 7:3.

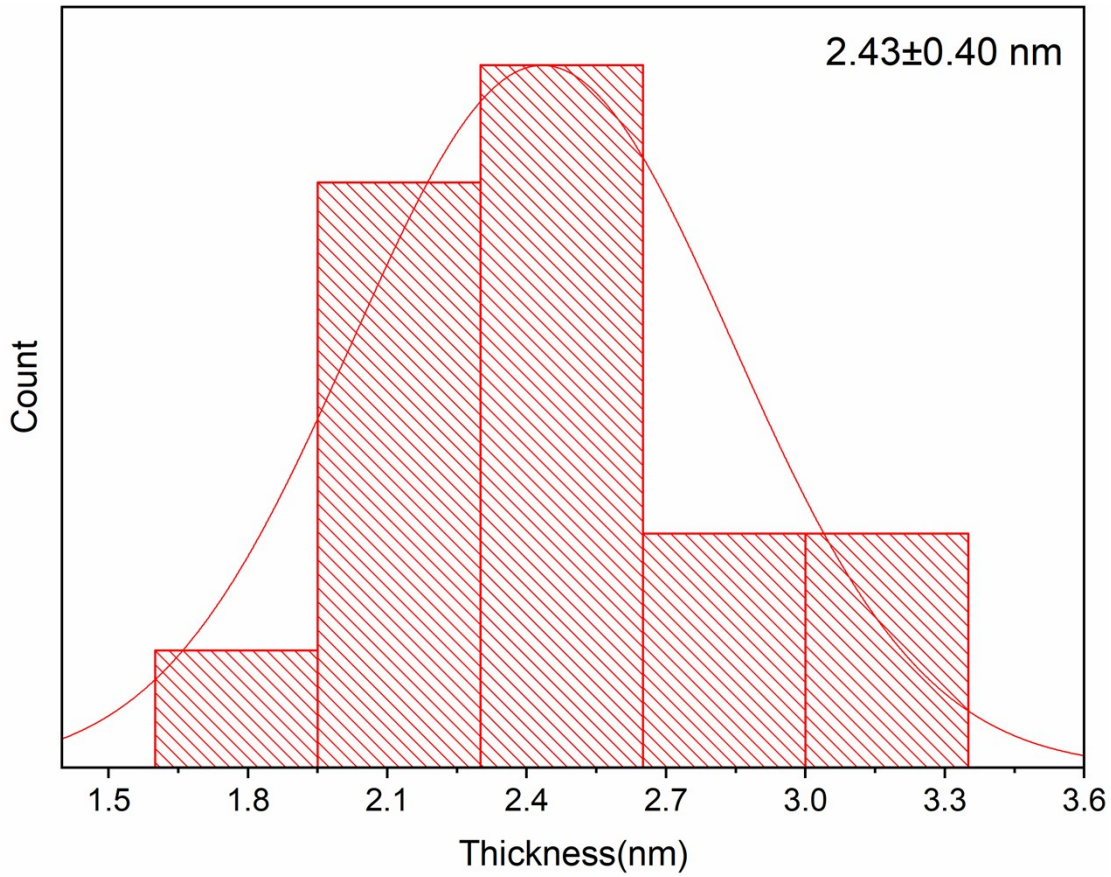

Figure S2. The thickness distribution of Mn-doped $CsPbCl_3$ NPLs at Mn-Pb feed ratio of 7:3.

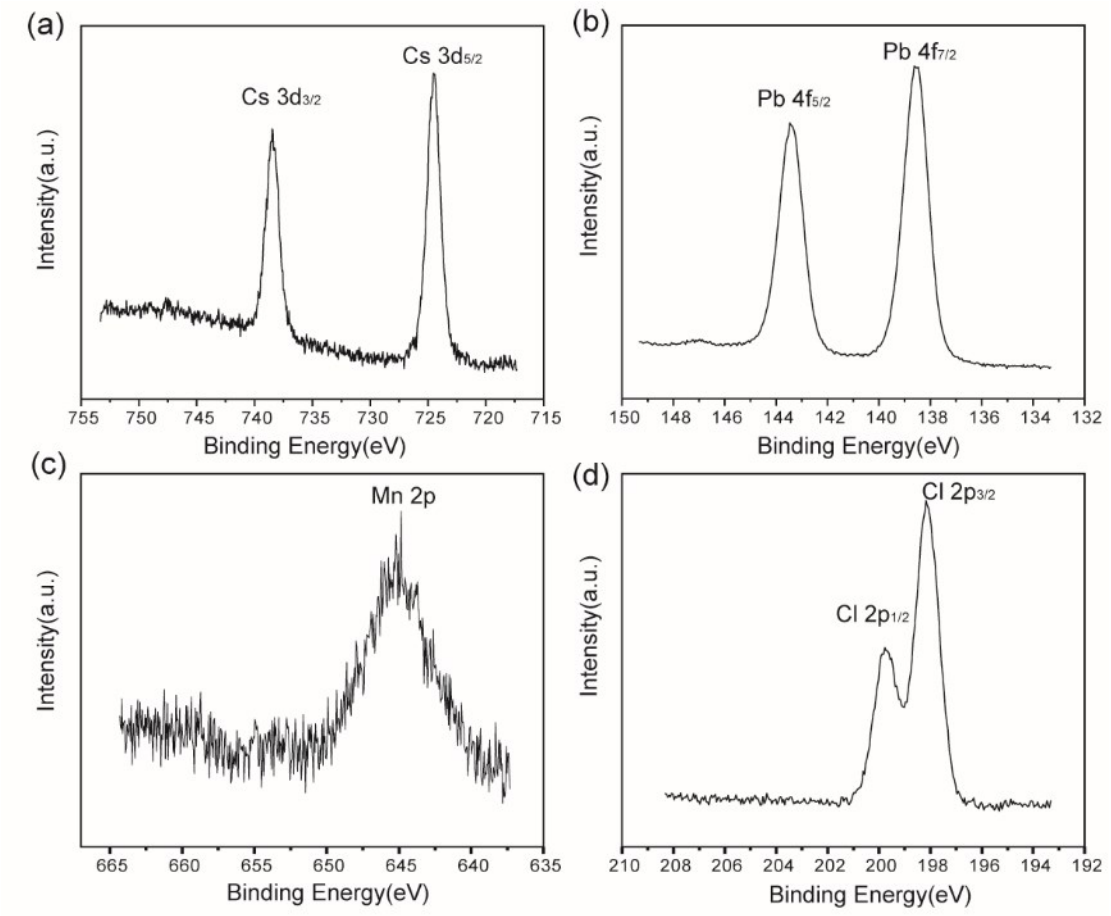

Figure S3. HRXPS spectra for Mn-doped $CsPbCl_3$ NPLs. The HRXPS spectrum of Cs 3d in **(a)** shows two symmetric peaks attributed to Cs $3d_{3/2}$ and Cs $3d_{5/2}$ with binding energies of 738.4 eV and 724.4 eV, respectively. The Pb 4f spectrum in **(b)** exhibits two symmetric peaks at 138.6 eV and 143.4 eV, which correspond to Pb $4f_{7/2}$ and Pb $4f_{5/2}$, respectively, with a spin-orbit splitting energy of 4.8 eV, suggesting that Pb is present in a nearly identical coordination environment with the Pb^{2+}. The binding energy at 645.2 eV in **(c)** is consistent with Mn 2p, which further proves the success of Mn doping. To further confirm the chemical bond configuration of the element, the bonding states of Cl was investigated. As shown in **(d)**, the Cl 2p peaks can be fitted into two peaks at binding energies 199.7 eV and 198.1 eV, which correspond to the inner and surface Cl^-, respectively.

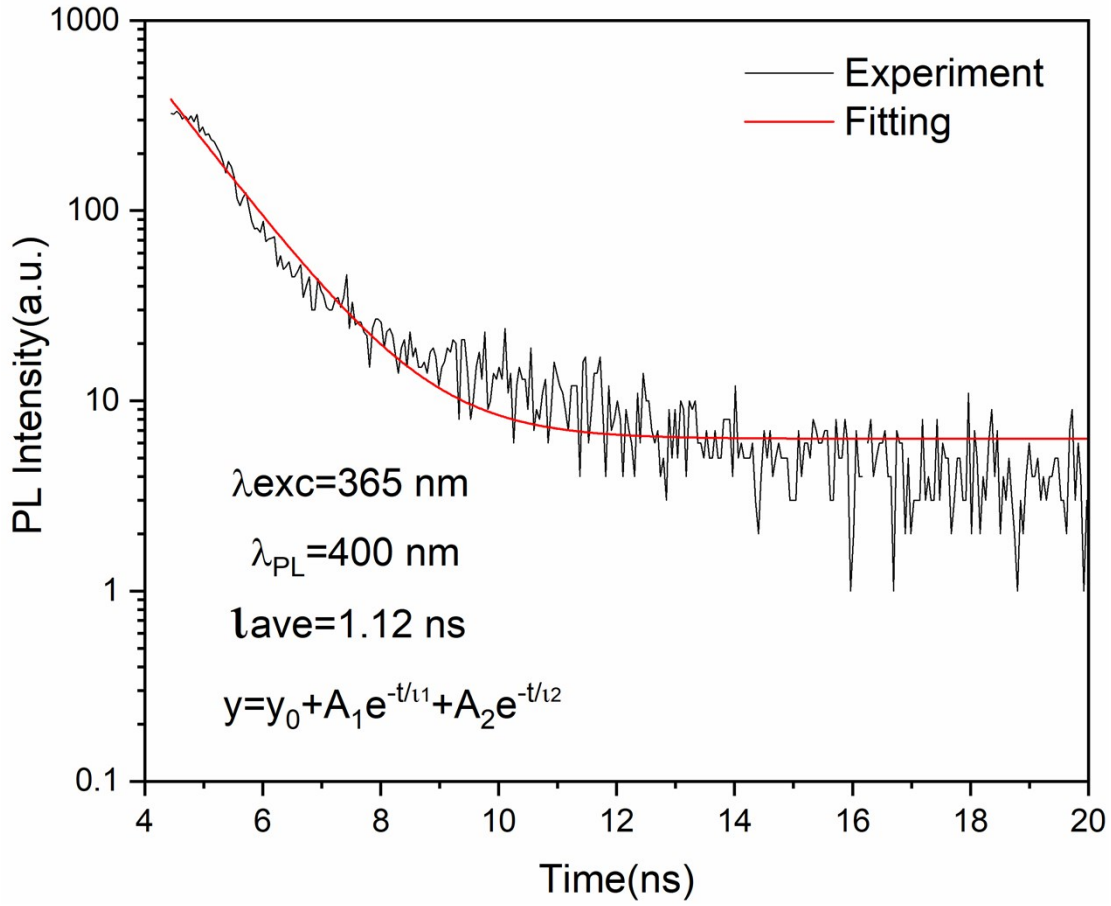

Figure S4. PL decay dynamics of excitonic emission from $CsPbCl_3$ NPLs at Mn-Pb feed ratio of 7:3 with excitation wavelength at 365 nm.

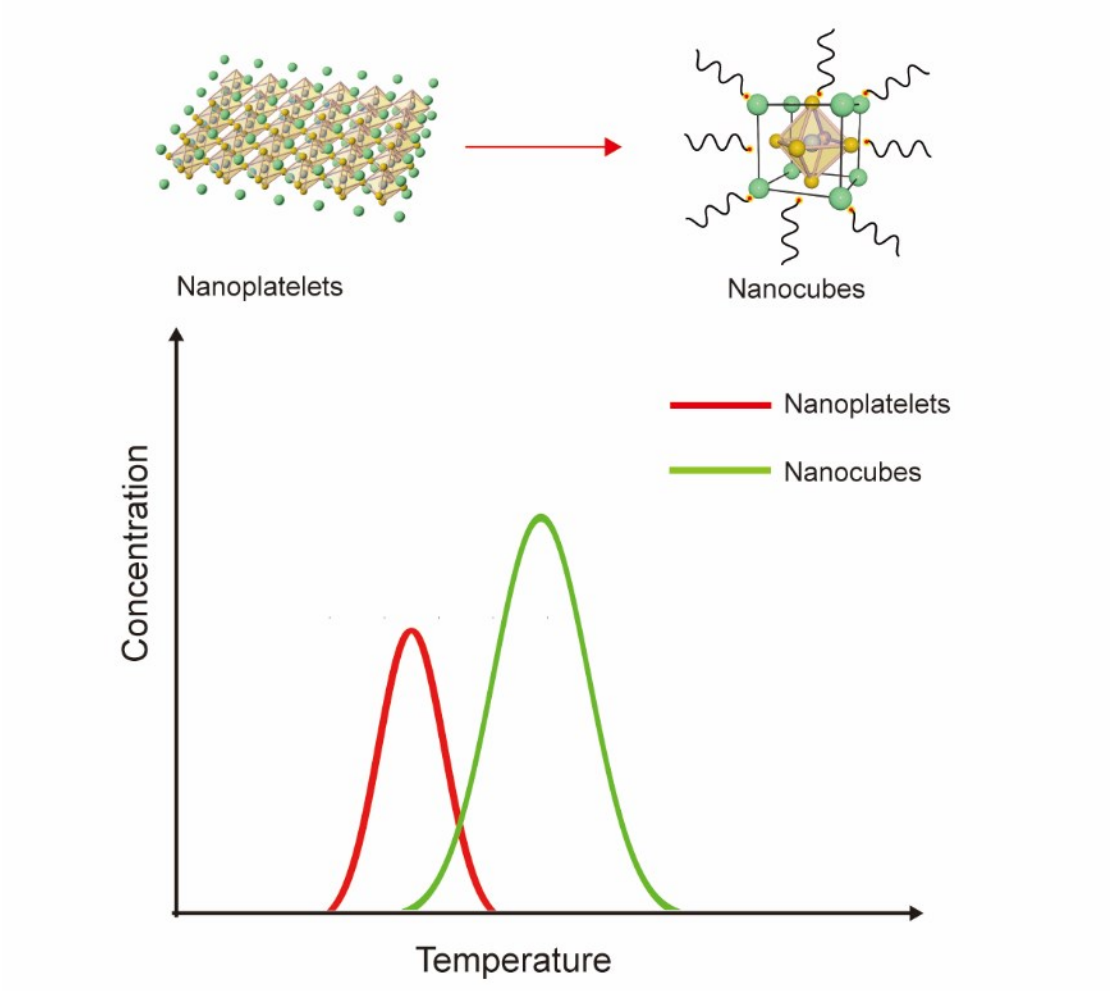

Figure S5. The proposed growth mechanism about the influence of the temperature on the Mn-doped $CsPbCl_3$ nanocrystals.

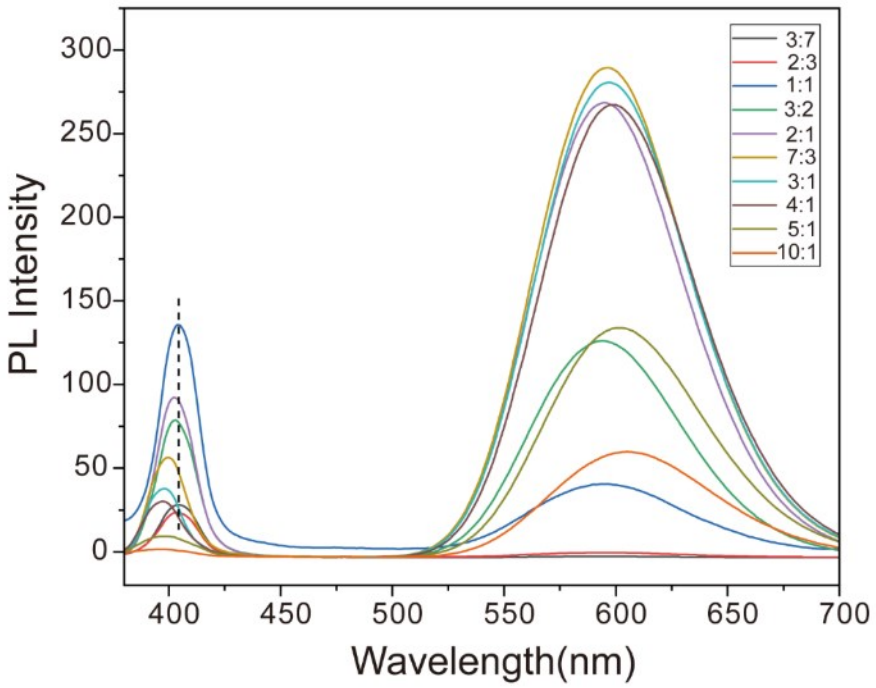

Figure S6. The non-normalized PL spectra for different Mn-Pb feed ratios.

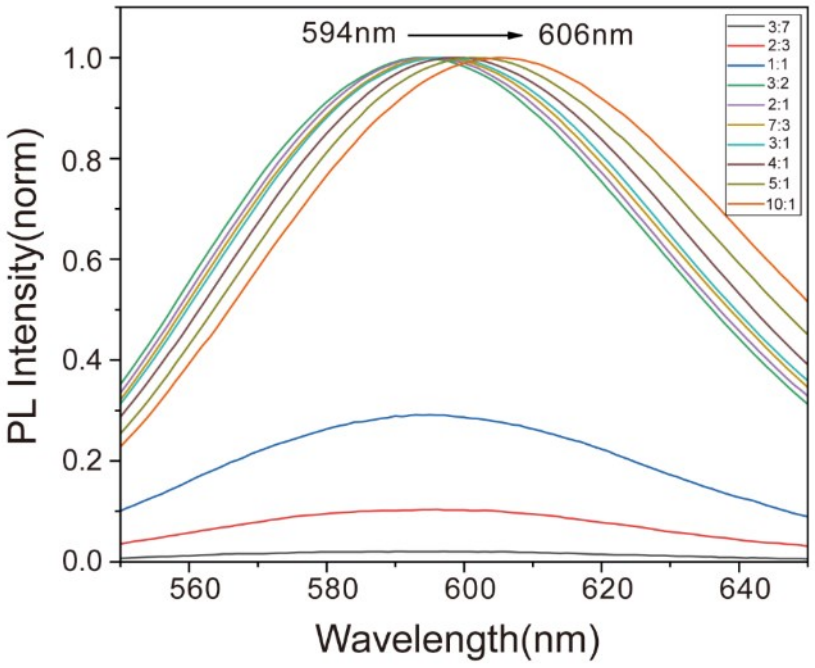

Figure S7. The normalized PL spectra of Figure 3a around at 600 nm for different Mn-Pb feed ratios.

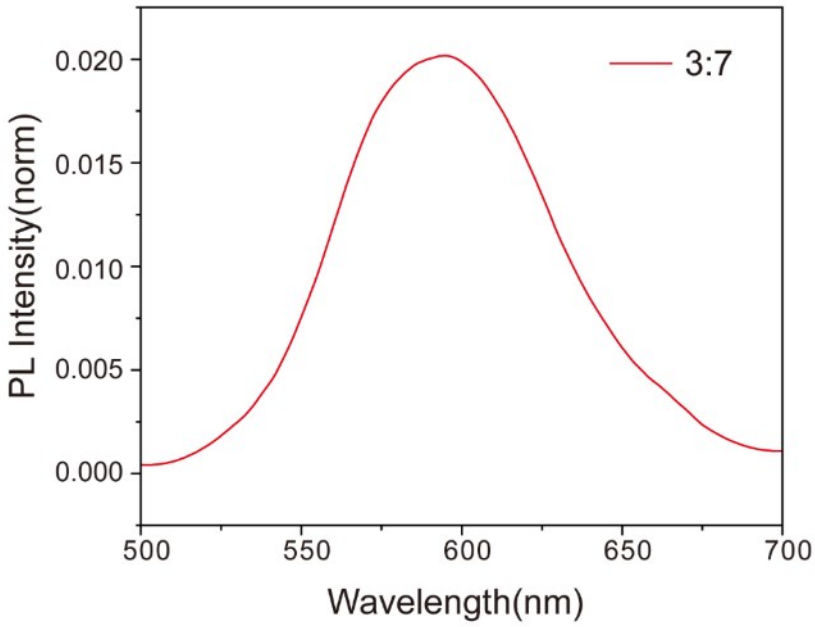

Figure S8. The normalized PL spectrum of Figure 3a around at 600 nm at Mn-Pb feed ratio of 3:7.

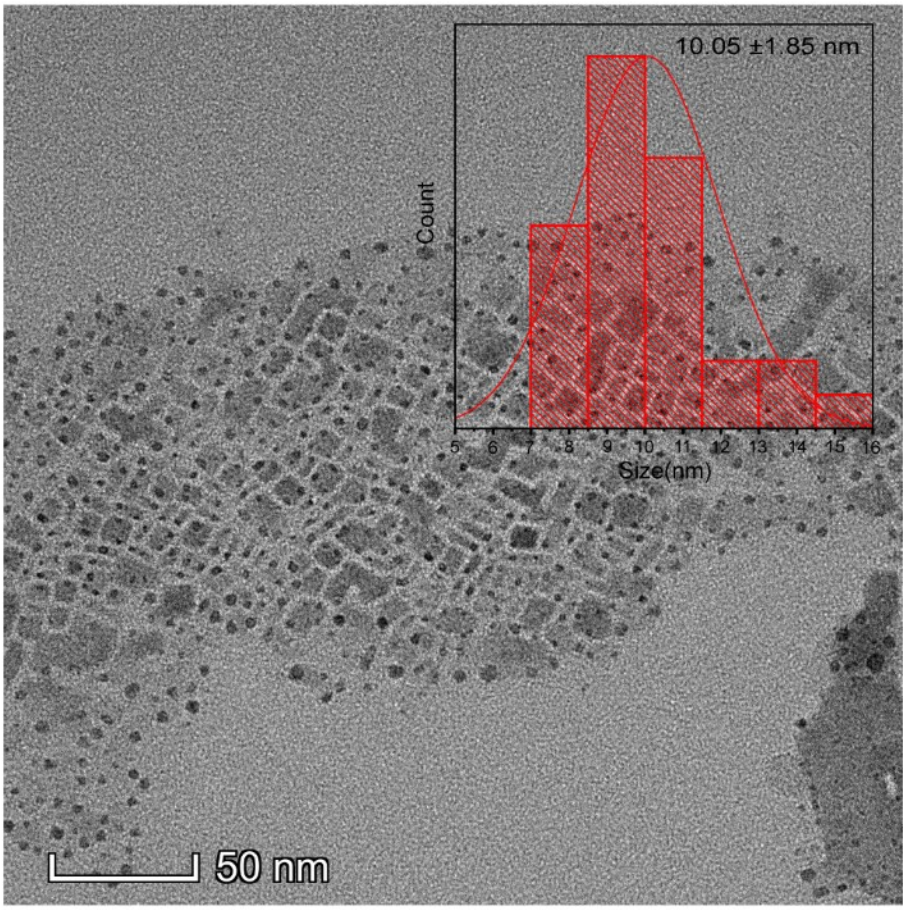

Figure S9. TEM image and size distribution of undoped $CsPbCl_3$ nanocrystals.

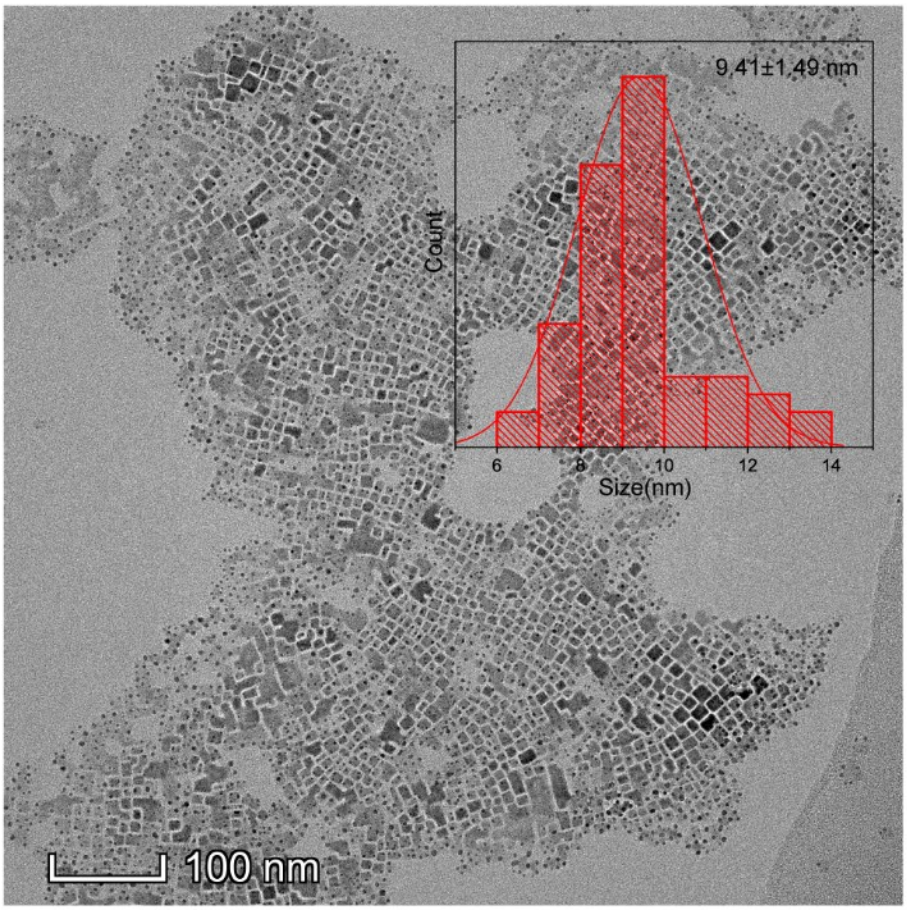

Figure S10. TEM image and size distribution of Mn-doped $CsPbCl_3$ nanocrystals with Mn: Pb=3:7.

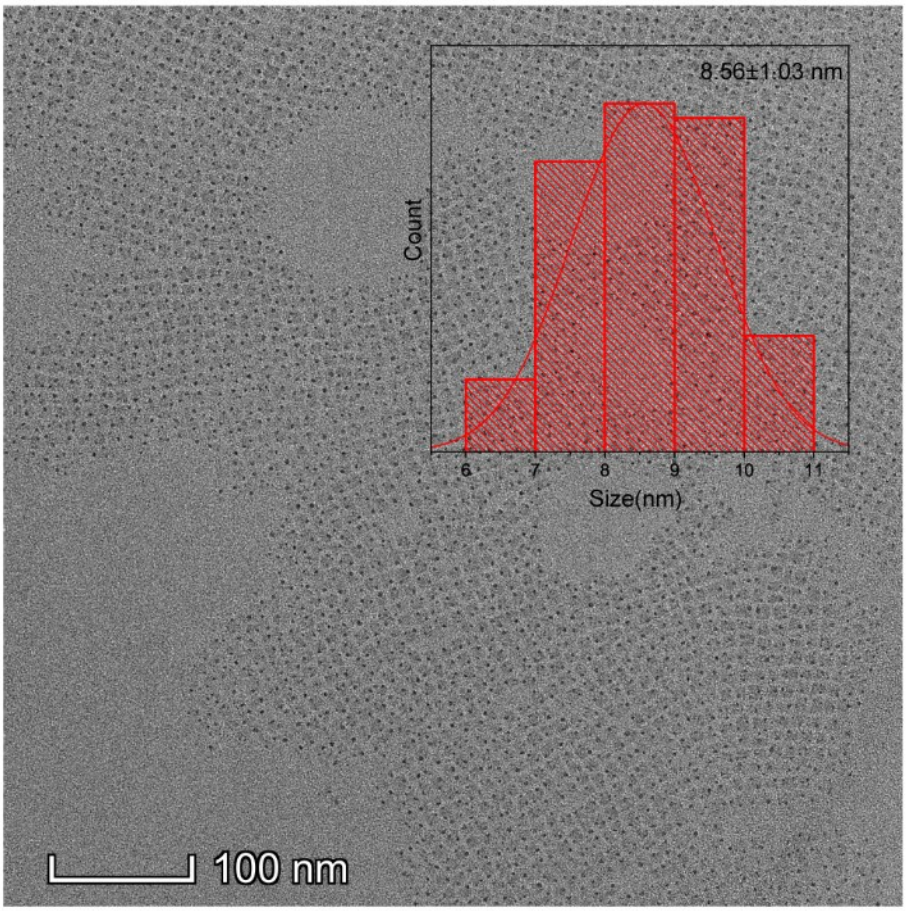

Figure S11. TEM image and size distribution of Mn-doped $CsPbCl_3$ nanocrystals with Mn: Pb=2:3.

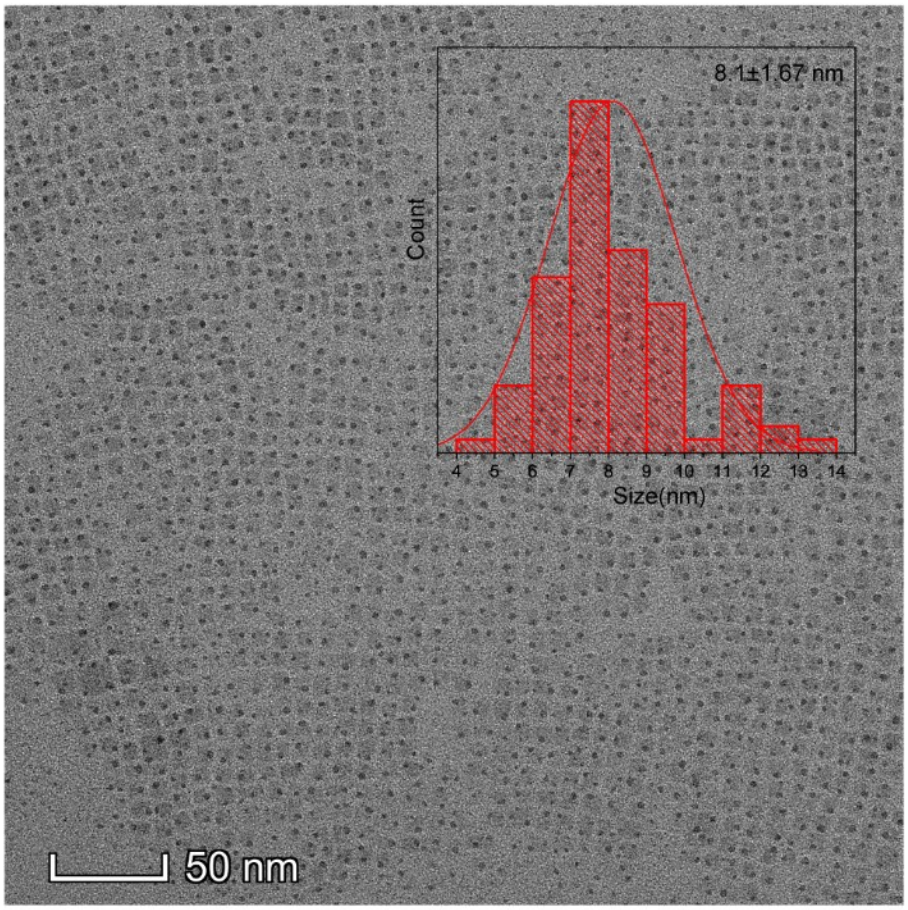

Figure S12. TEM image and size distribution of Mn-doped $CsPbCl_3$ nanocrystals with Mn: Pb=1:1.

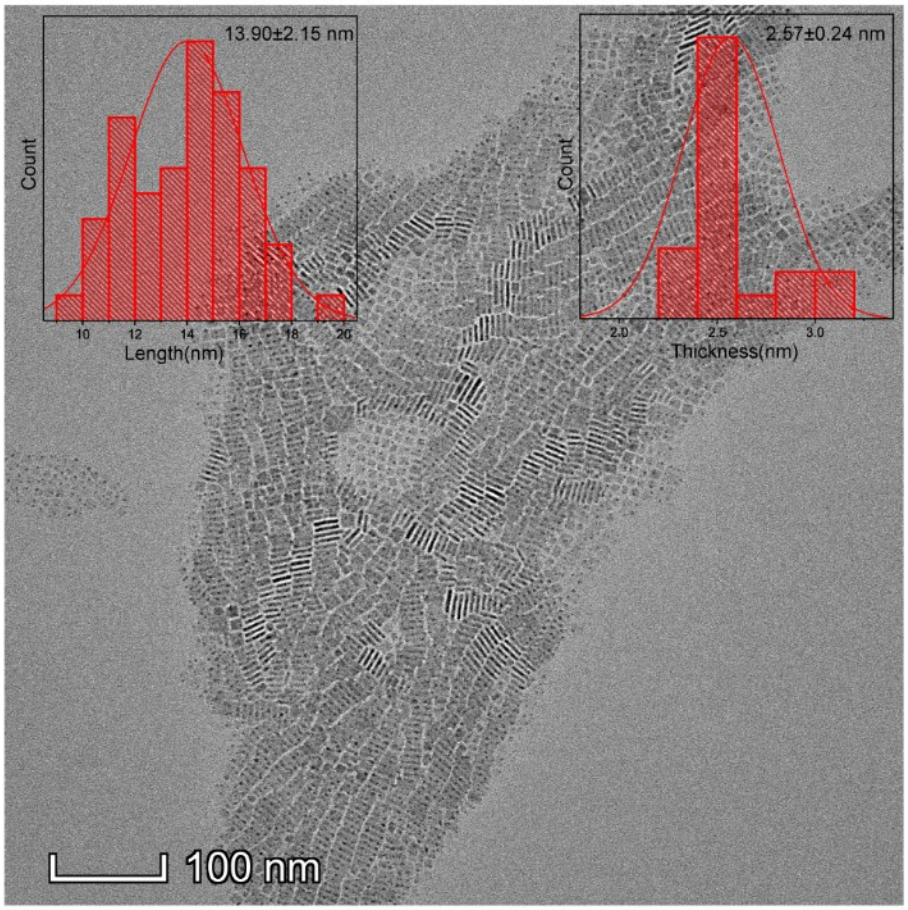

Figure S13. TEM image, length and thickness distributions of Mn-doped $CsPbCl_3$ nanocrystals with Mn: Pb=3:2.

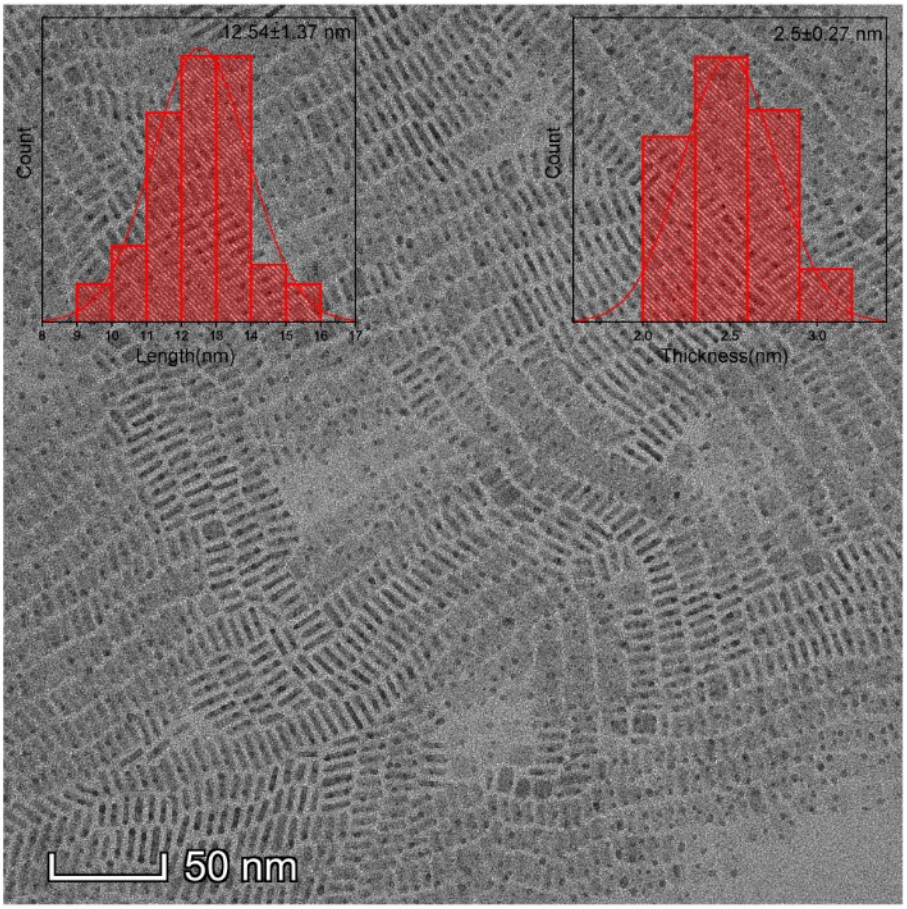

Figure S14. TEM image, length and thickness distributions of Mn-doped $CsPbCl_3$ nanocrystals with Mn: Pb=2:1.

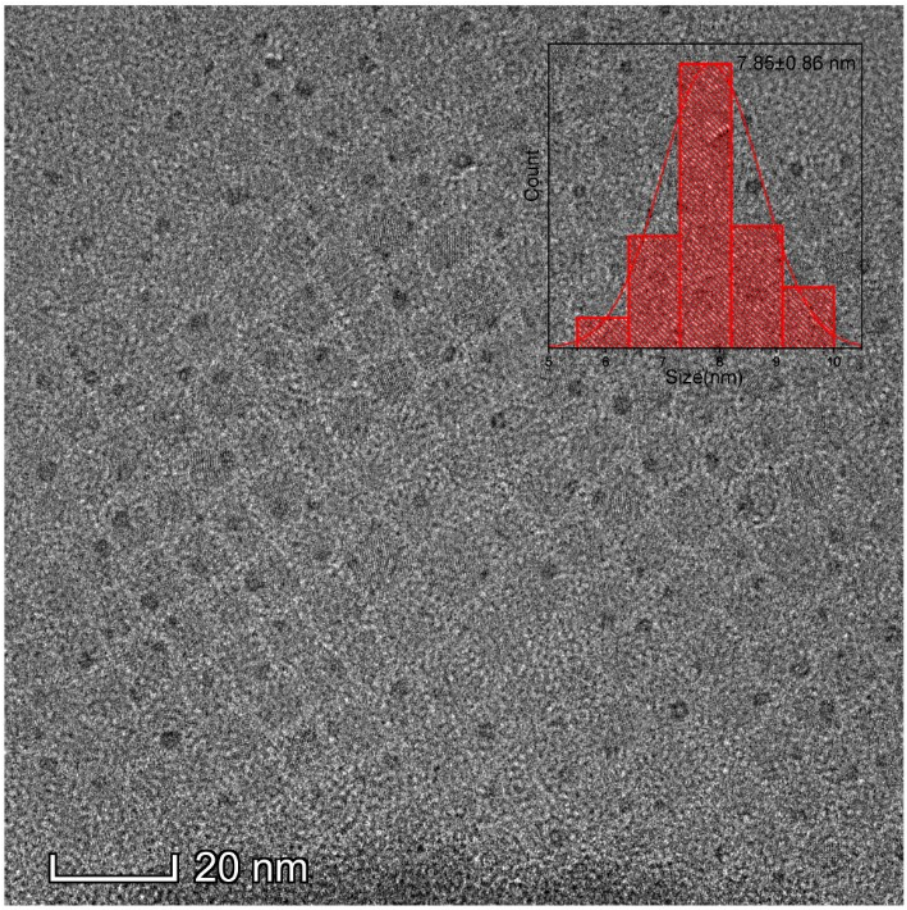

Figure S15. TEM image and size distribution of Mn-doped $CsPbCl_3$ nanocrystals with Mn: Pb=2:1.

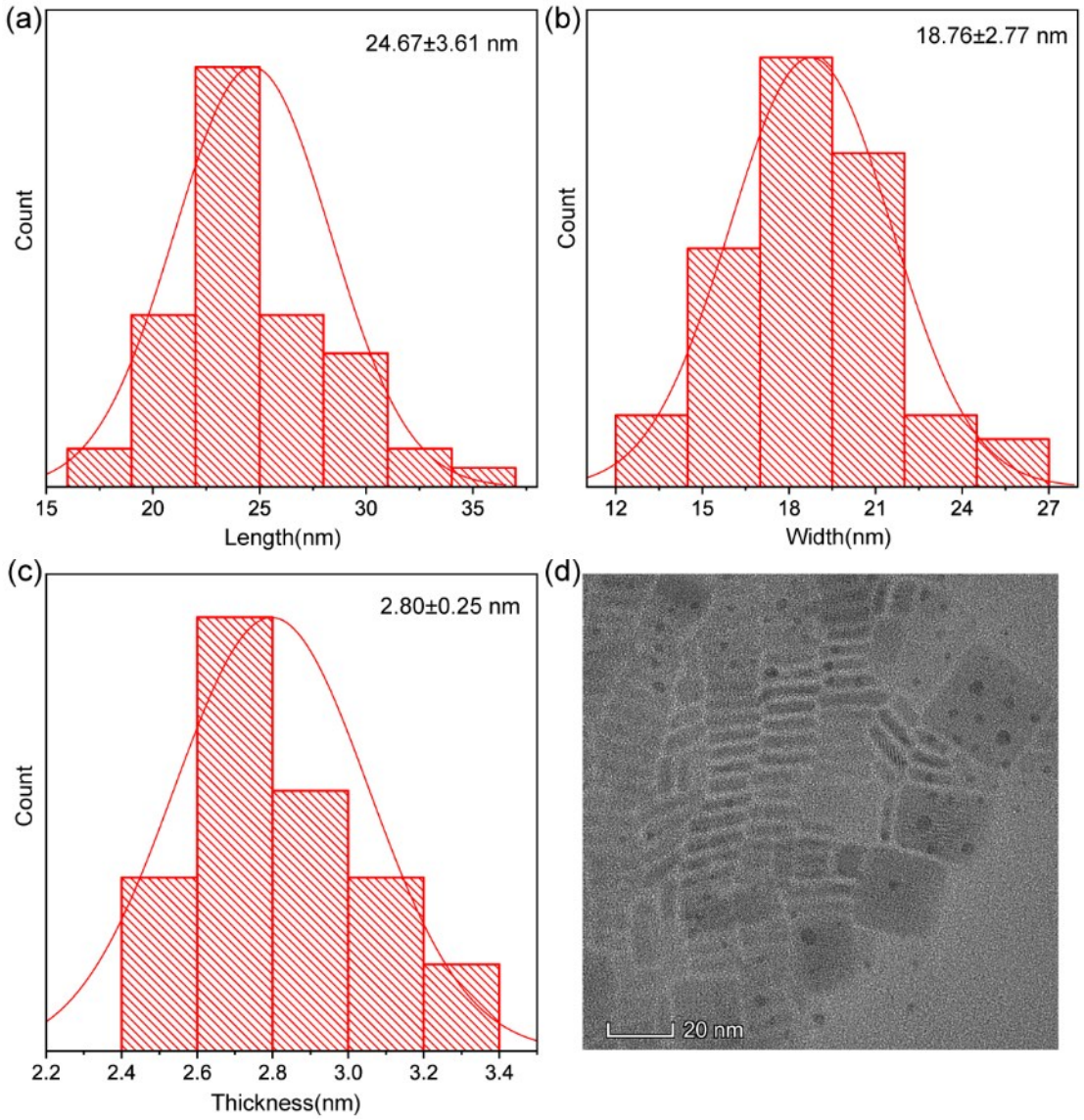

Figure S16. TEM image and size distributions of Mn-doped $CsPbCl_3$ nanocrystals with Mn: Pb=3:1.

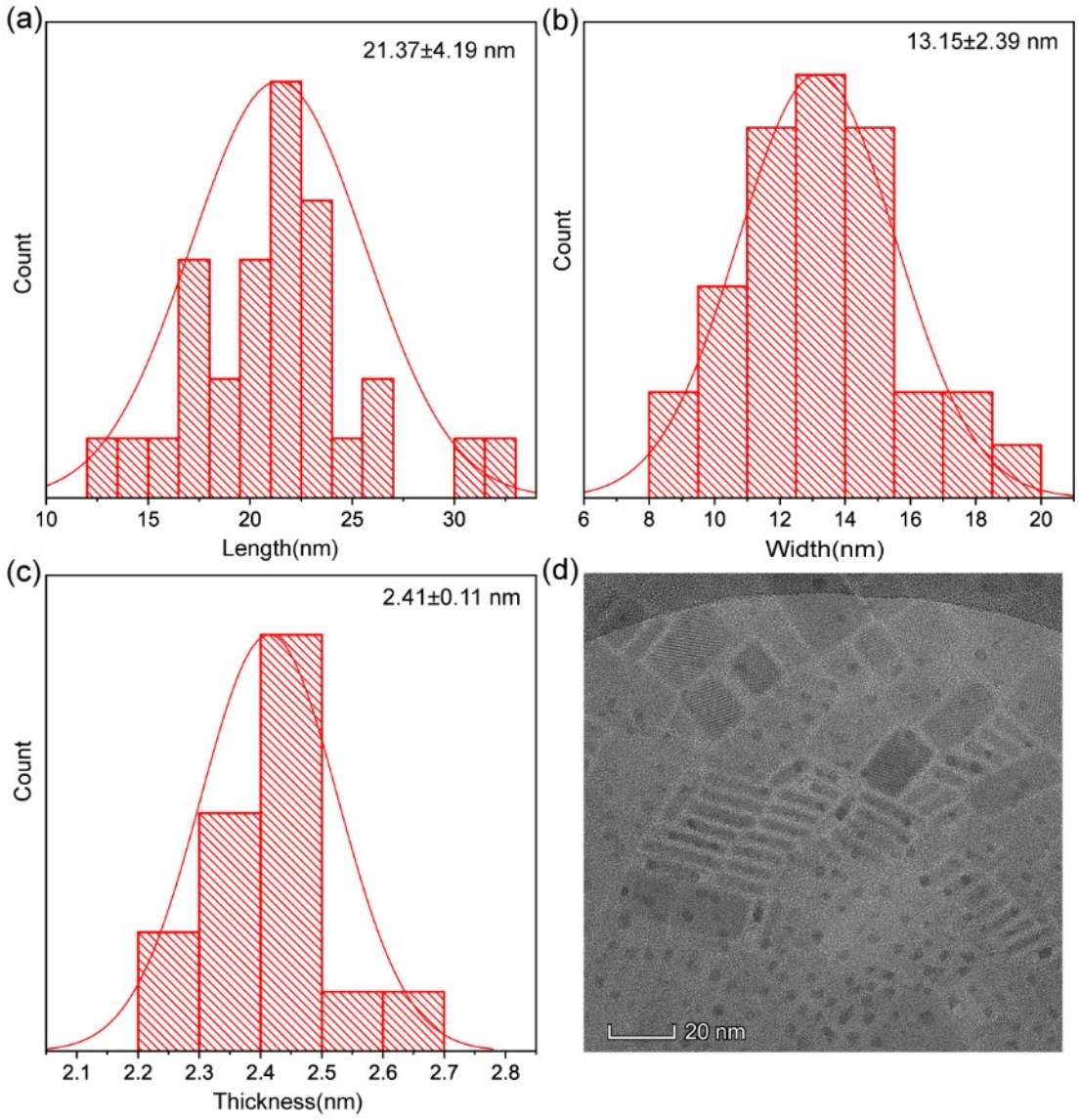

Figure S17. TEM image and size distributions of Mn-doped $CsPbCl_3$ nanocrystals with Mn: Pb=4:1.

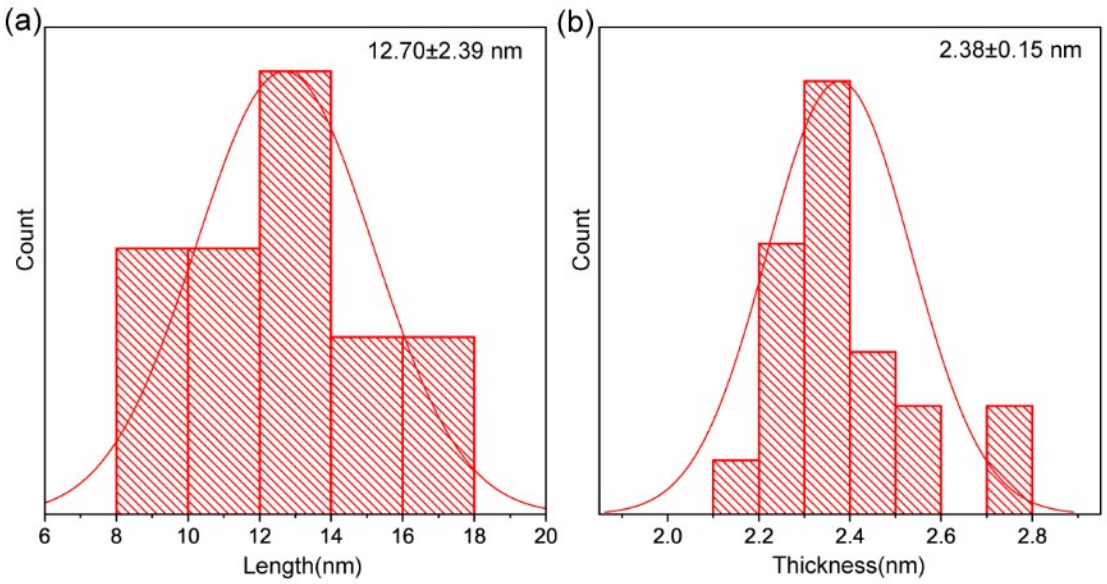

Figure S18. Length and thickness distributions of Mn-doped $CsPbCl_3$ nanocrystals with Mn: Pb=5:1.

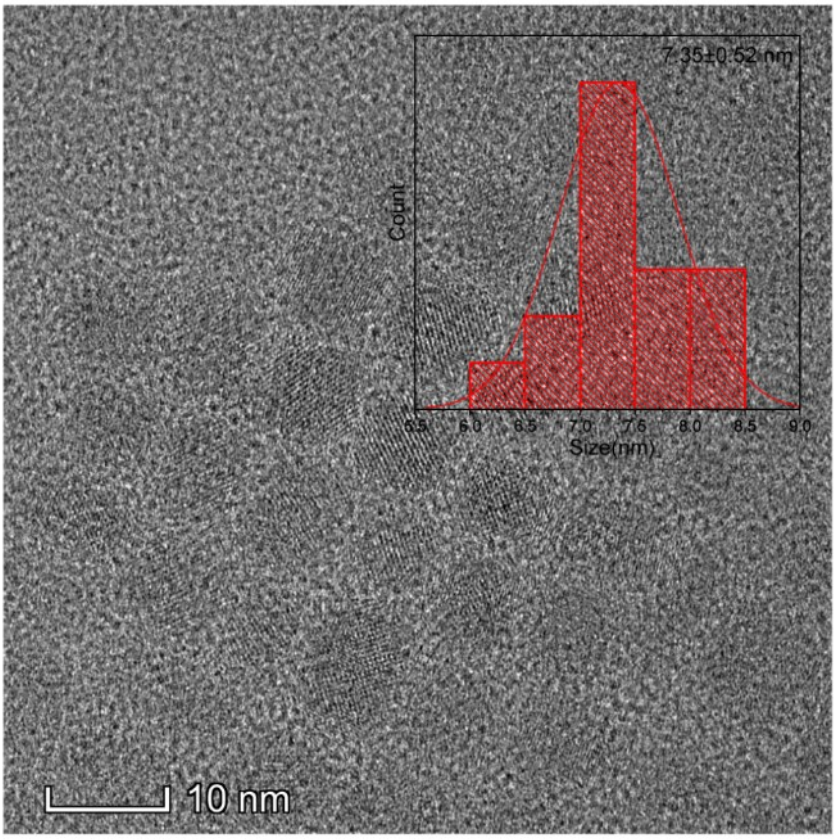

Figure S19. TEM image and size distribution of Mn-doped $CsPbCl_3$ nanocrystals with Mn: Pb=5:1.

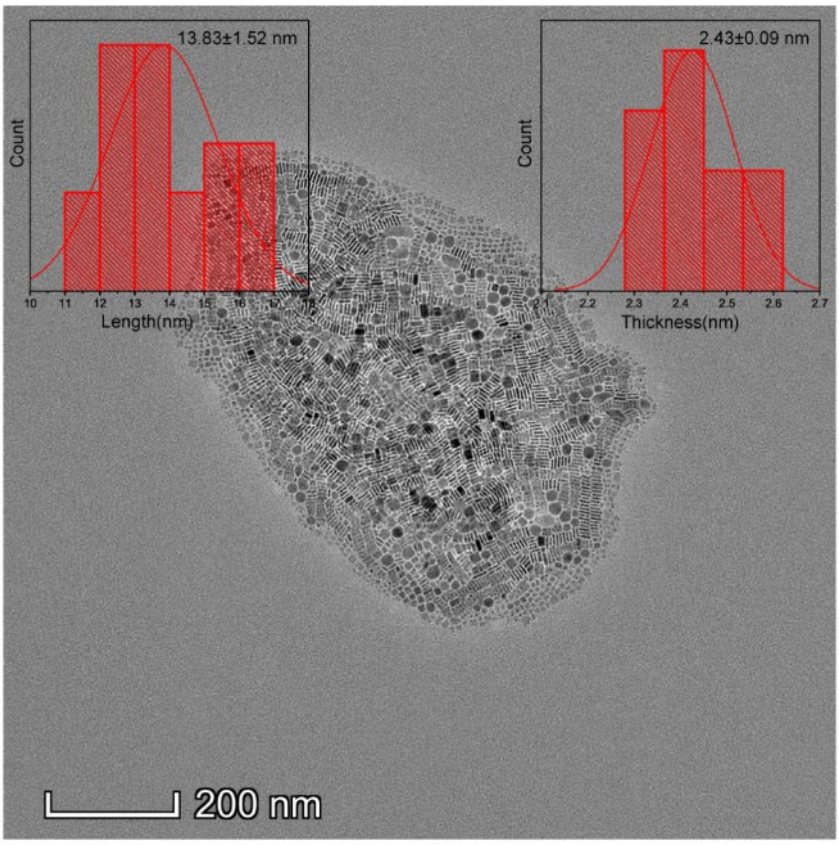

Figure S20. TEM image and size distributions of Mn-doped $CsPbCl_3$ nanocrystals with Mn: Pb=10:1.

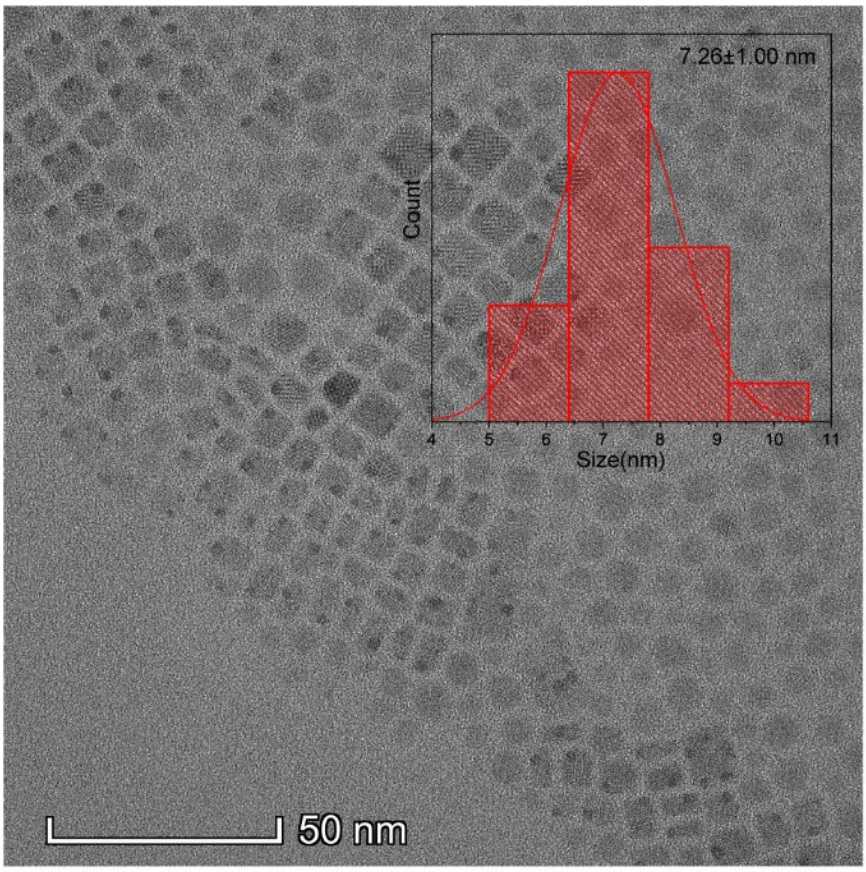

Figure S21. TEM image and size distribution of Mn-doped $CsPbCl_3$ nanocrystals with Mn: Pb=10:1.

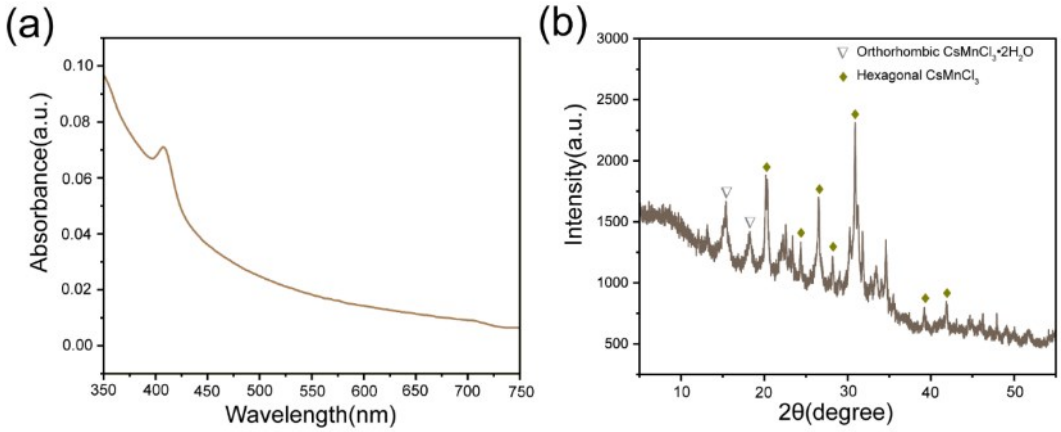

Figure S22. (a) UV-vis spectrum and (b) XRD pattern of the $CsMnCl_3$ products.

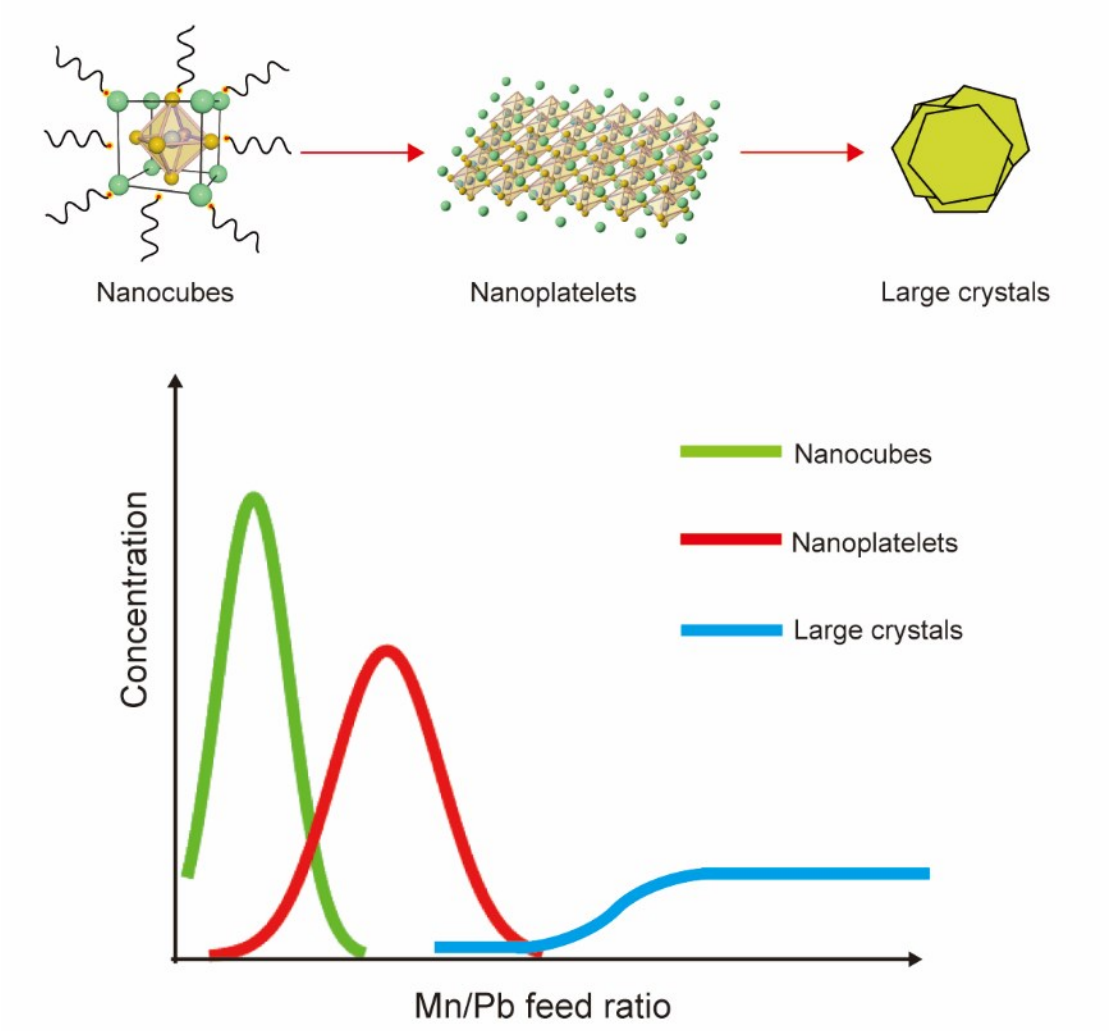

Figure S23. The proposed growth mechanism of the Mn-doped $CsPbCl_3$ nanocrystals as a function of Mn-Pb feed ratio.

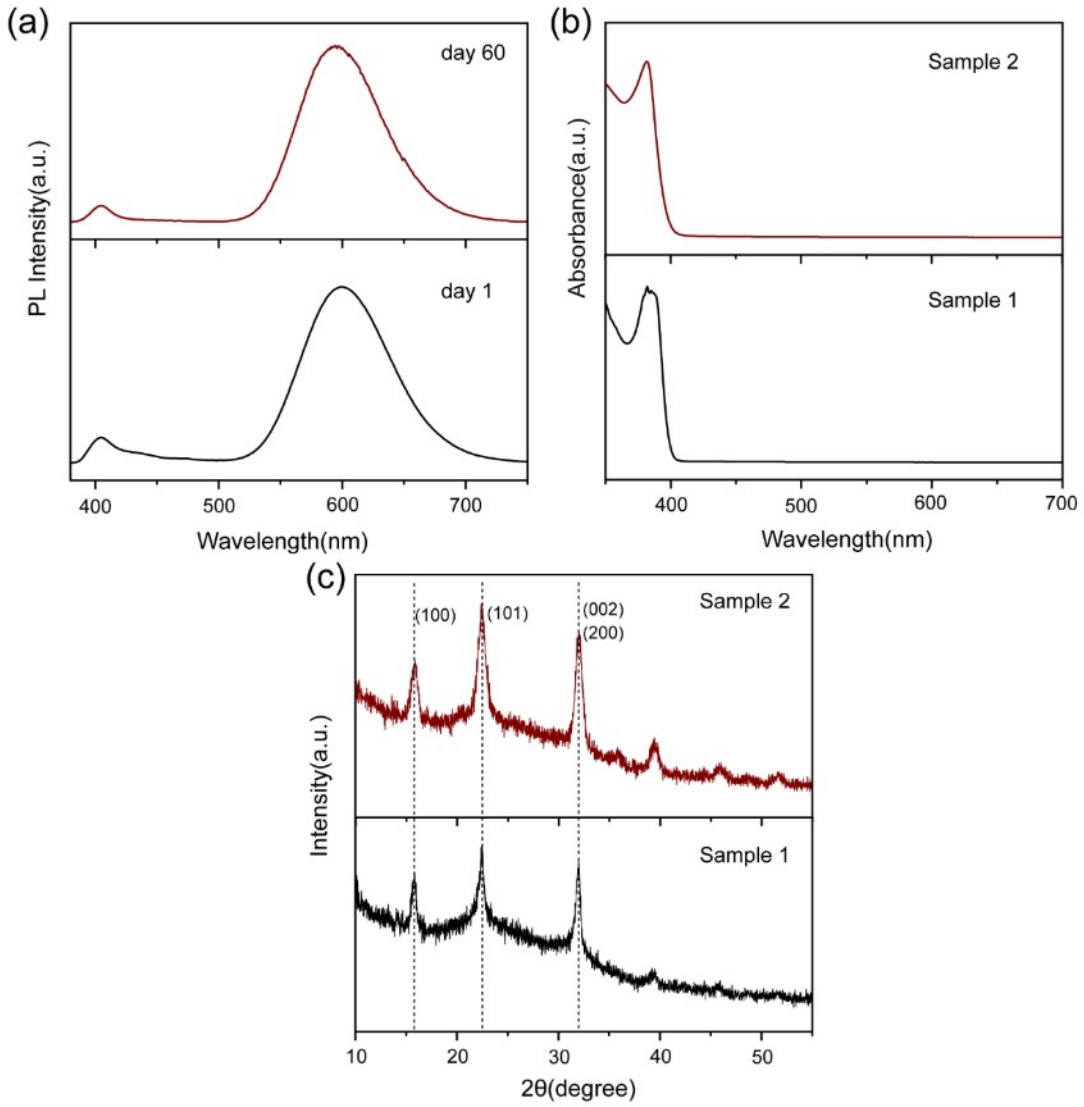

Figure S24. (a)The optical stability and (b)-(c) experimental repeatability.

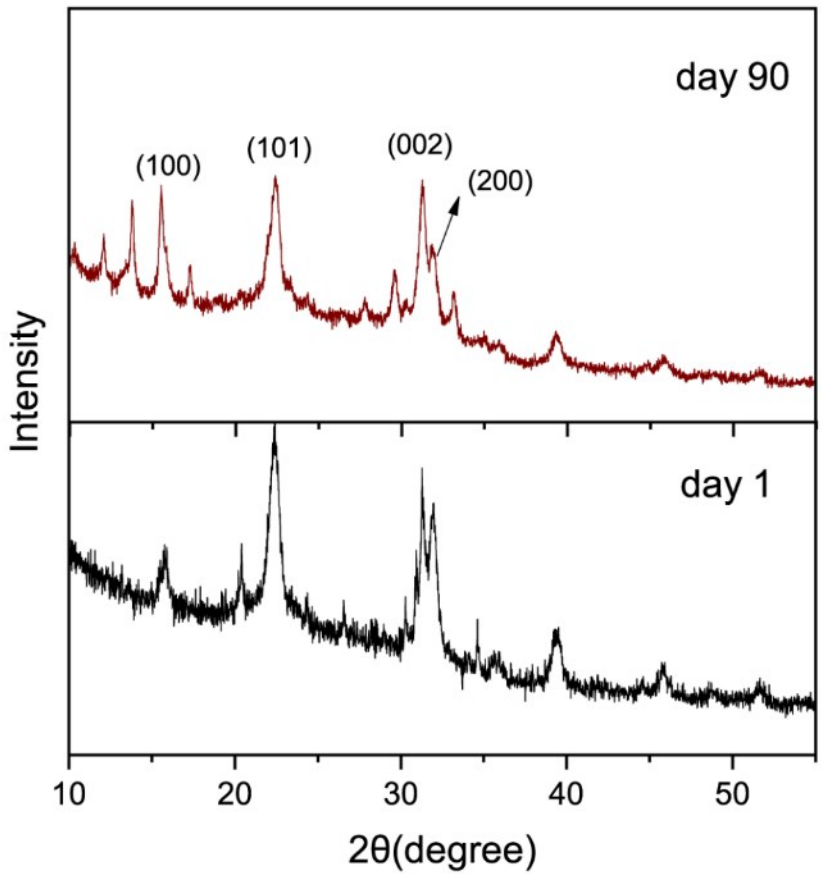

Figure S25. The XRD of Mn-doped NPLs after 90 days in air.

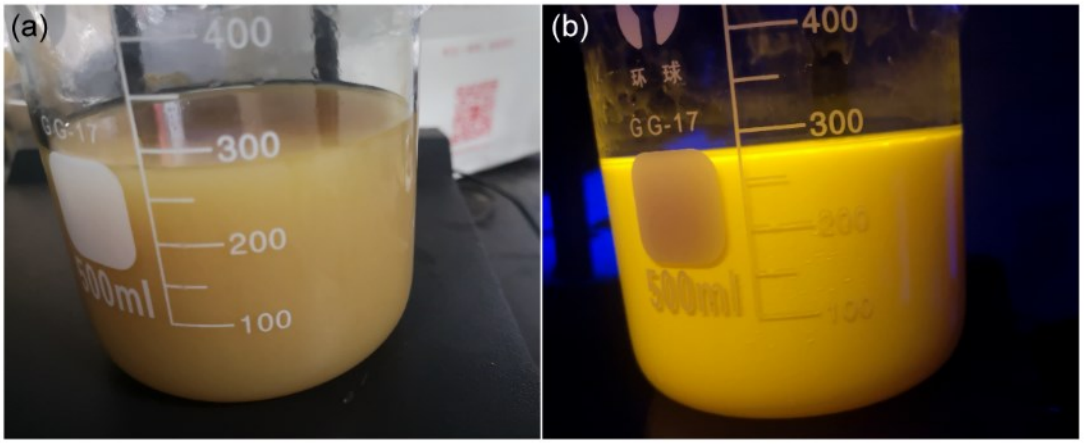

Figure S26. Digital images of the freshly prepared Mn-doped NPLs solution under natural light (a) and UV light (b).

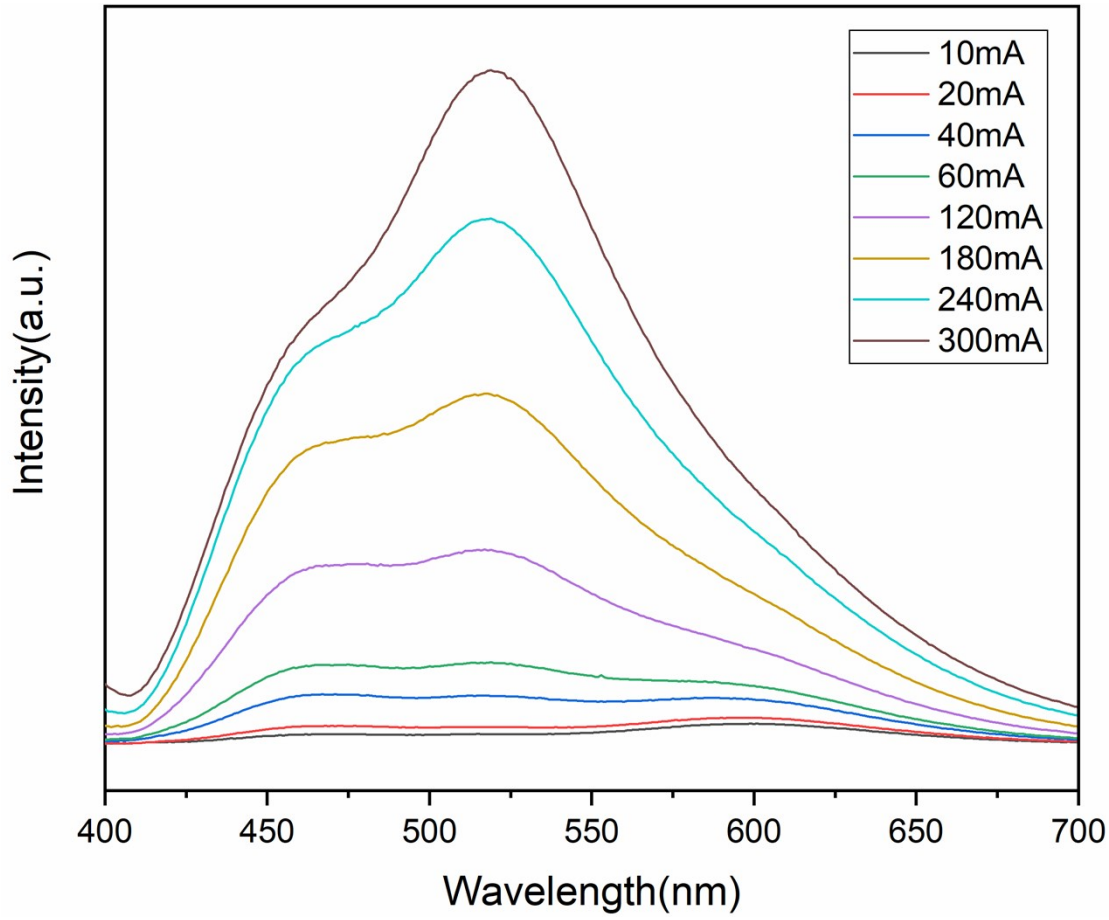

Figure S27 The EL spectra of the WLED operated at different forward-bias current.

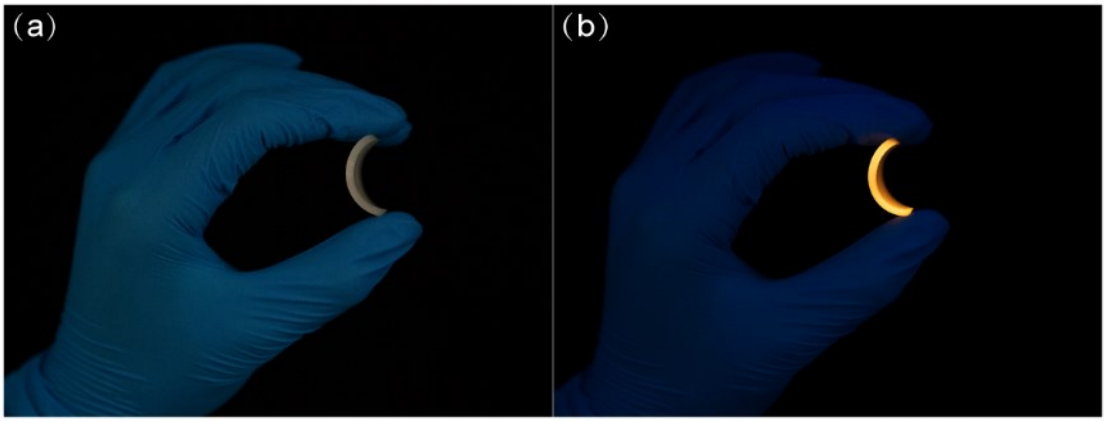

Figure S28.The flexible composite film under natural light (a) and UV light (b) after 6 months.

Table S1. The Mn substitution ratio of the $CsPb_xMn_{1-x}Cl_3$ nanocrystals characterized by ICP-OES for different Mn-Pb molar feed ratios.

Mn-Pb feed ratio (proportion)	Actual ratio of Mn/(Mn+Pb) (%)
3:7 (30%)	0.4
2:3 (40%)	0.47
1:1 (50%)	0.52
3:2 (60%)	0.53
2:1 (66.7%)	2.83
7:3 (70%)	1.23
3:1 (75%)	4.26
4:1 (80%)	8.28
5:1 (83.3%)	6.5
10:1 (90.9%)	44.73

Table S2. PLQYs of typical Mn-doped $CsPbX_3$ nanoplatelets

Mn-doped $CsPbX_3$ nanoplatelets	PL peak (exciton/Mn)	PLQYs	Method	Temperature	Ref.
Mn-doped $CsPbCl_3$	400nm/586nm	20.3%		Room-temperature	1
Mn-doped $CsPbCl_3$	~400nm/~585nm	27%	Hot injection	180 ℃	2
Mn-doped $CsPbCl_3$	392nm/577nm	22.2%	Solvothermal	120 ℃	3
Mn-doped $CsPbCl_3$	391nm/~600nm	20.8%	Solvothermal	200 ℃	4
Mn-doped $CsPbBr_3$	462nm/600nm	--	Postsynthesis	RT	5
Mn-doped $CsPbCl_3$	400nm/596nm	53.76%	Non-hot-injection	100 ℃	Our work

References

1. W. J. Mir, M. Jagadeeswararao, S. Das and A. Nag, *ACS Energy Lett.*, 2017, **2**, 537-543.

2. S. D. Adhikari, S. K. Dutta, A. Dutta, A. K. Guria and N. Pradhan, *Angew. Chem. Int. Ed.*, 2017, **56**, 8746-8750.

3. C. Liu, J. Lin, W. Zhai, Z. Wen, X. He, M. Yu, Y. Huang, Z. Guo, C. Yu and C. Tang, *RSC Adv.*, 2019, **9**, 39315.

4. Z. Li, E. Hofman, A. H. Davis, A. Khammang, J. T. Wright, B. Dzikovski, R. W. Meulenberg and W. Zheng, *Chem. Mater.*, 2018, **30**, 6400-6409.

5. W. J. Mir, Y. Mahor, A. Lohar, M. Jagadeeswararao, S. Das, S. Mahamuni and A. Nag, *Chem. Mater.*, 2018, **30**, 8170-8178.